Temporal Interactions during Paired-Electrode Stimulation in Two Retinal Prosthesis Subjects

Alan Horsager,[1,2] *Geoffrey M. Boynton,*[3] *Robert J. Greenberg,*[4] *and Ione Fine*[3]

Purpose. Since 2002, six blind patients have undergone implantation of an epiretinal 4 × 4 electrode array designed to directly stimulate the remaining cells of the retina after severe photoreceptor degeneration due to retinitis pigmentosa. This study was conducted to investigate how the brightness of percepts is affected by pulse timing across electrodes in two of these patients.

Methods. Subjects compared the perceived brightness of a standard stimulus (synchronous pulse trains presented across pairs of electrodes) to the perceived brightness of a test stimulus (pulse trains across the electrode pair phase shifted by 0.075, 0.375, 1.8, or 9 ms). The current amplitude necessary for each phase-shifted test stimulus to match the brightness of the standard was determined.

Results. Depending on the electrode pair, interactions between electrodes were either facilitatory (the perceived brightness produced by stimulating the pair of electrodes was greater than that produced by stimulating either electrode alone) or suppressive (the perceived brightness produced by stimulating the pair of electrodes was less than that produced by stimulating either electrode alone). The amount of interaction between electrodes decreased as a function of increased separation both in time (the phase-shift between pulse trains) and space (center-to-center distance between the electrode pair).

Conclusions. For visual prostheses to represent visual scenes that are changing in both space and time requires the development of spatiotemporal models describing the effects of stimulation across multiple electrodes. During multielectrode stimulation, interactions between electrodes have a significant influence on subjective brightness that includes both facilitatory and suppressive effects, and these interactions can be described with a simple computational model. (ClinicalTrials.gov number, NCT00279500.) (*Invest Ophthalmol Vis Sci.* 2011;52:549–557) DOI:10.1167/iovs.10-5282

From the [1]Neuroscience Graduate Program and the [2]Institute for Genetic Medicine, University of Southern California, Los Angeles, California; the [3]Department of Psychology, University of Washington, Seattle, Washington; and [4]Second Sight Medical Products, Inc., Sylmar, California.

Supported by Second Sight Medical Products, Inc., the Fletcher Jones Foundation, the National Institutes of Health (NEI EY012893 EY014645), and Research to Prevent Blindness. AH received graduate student support from Second Sight Medical Products Inc., during the period in which this research was conducted.

Submitted for publication January 27, 2010; revised April 30 and July 12, 2010; accepted July 21, 2010.

Disclosure: **A. Horsager**, Second Sight Medical Products, Inc. (F), P; **G.M. Boynton**, P; **R.J. Greenberg**, Second Sight Medical Products Inc. (E, I), P; **I. Fine**, P

Corresponding author: Alan Horsager, Institute for Genetic Medicine, 2250 Alcazar Street, Room 256, Los Angeles, CA 90033; horsager@usc.edu.

Retinitis pigmentosa (RP) and age-related macular degeneration (AMD) are photoreceptor diseases that cause substantial vision loss or blindness in more than 15 million people worldwide.[1–4] In both diseases, after the loss of the photoreceptor layer, the spatial organization of the inner nuclear and ganglion cell layers can become disrupted and the inner nuclear and ganglion cell layers begin to thin[5,6] (but see also Ref. 7). However, inner nuclear and ganglion cell layers maintain relatively high cell density,[7–9] and some functional circuitry remains.[10–12] These findings of residual structure and function within the inner layers of the diseased retina have inspired research focused on sight restoration technologies that interface with the remaining retinal cells.

Although a variety of techniques, such as gene replacement therapy,[13–17] engineered photo-gates,[18–20] and light-sensitive proteins such as channelrhodopsin-2 (ChR2) [10,21–24] are currently being developed, all have some limitations in scope. Gene therapies require the maintenance of photoreceptors[6] and are specific to a single gene mutation.[25] ChR2 activation requires light stimulation levels that are five orders of magnitude greater than the threshold of cone photoreceptors[26] and have limited dynamic range.[27]

Several research groups are in the process of developing microelectronic retinal prostheses with the ultimate goal of restoring vision in blind subjects by stimulating the remaining retinal cells with spatiotemporal sequences of electrical pulses. Analogous to cochlear implants, these devices are designed to directly stimulate remaining retinal neurons with pulsing electrical current. To date, both semiacute and long-term implanted devices have been demonstrated to be safe and capable of generating visual percepts in human subjects.[28–36]

The ultimate goal of these prostheses is to generate useful vision in blind patients by presenting a spatiotemporal sequence of electrical pulses that produce percepts that represent meaningful visual information. To achieve this goal, it is necessary to develop predictive models that can determine which stimulation pattern will produce percepts with brightness and shape that best represent a given region of the visual scene. Over the past several years, our group has begun to develop such models using data from six patients who underwent implantation of an epiretinal prosthesis containing 16 electrodes. This work provides a proof-of-concept demonstration that predictive models can successfully describe patients' perceptual experiences. Our hope is that these models will also generalize, with modification, to the higher resolution arrays with smaller electrodes that are currently under trial or in development.[37]

Previous quantitative models from our group have been limited to describing the behavior of single electrodes. We have shown that the apparent brightness of percepts as a function of stimulation amplitude can be described as a power function closely analogous to the power function that can be used to predict apparent brightness as a function of light intensity in visually normal observers.[34,38] We have similarly shown that it is possible to predict the sensitivity of the human

visual system to a wide variety of retinal electrical stimulation patterns using a simple and biologically plausible model that shows some analogies to models used to describe temporal sensitivity to light in visually normal observers.[36,39]

However, extension of these single-electrode models to multielectrode stimulation is not necessarily straightforward. Significant spatiotemporal interactions are found between pairs or groups of electrodes, even when electrical field interactions are controlled for by phase-shifting pulses in time across the electrodes so that no pulse overlaps in time. These interactions seem to include both changes in brightness and changes in percept shape.[35] Similar results have been found for cochlear implants, where the precise timing of stimulation across electrodes has perceptual consequences as a result of both electrical field[40–42] and neuronal interactions.[43] Here we show that, although these interactions exist, the effects of spatiotemporal interactions between pairs of electrodes on percept brightness can be fit by a simple computational model.

Materials and Methods

Subjects

Data reported herein were collected from two patients with long-term implantation of 16-electrode retinal prostheses (Second Sight Medical Products, Inc., Sylmar, CA). These two patients, S05 and S06, were 59 and 55 years old, respectively, at the time of implantation (2004). Before surgery, subject S05 had bare light perception (BLP) in the implanted eye and subject S06 had no light perception (NLP). These two patients were a subset of six patients who have received the implants since February 2002. The other four patients were excluded from this study for a variety of reasons described elsewhere.[34]

All tests were performed after informed consent was obtained in a protocol approved by the Institutional Review Board at the Keck School of Medicine (University of Southern California, Los Angeles, CA) and according to the principles of the Declaration of Helsinki.

The Retinal Prosthesis

As described elsewhere,[36] the implants were placed epiretinally, with a 4×4 array of disc electrodes in the macular region (Fig. 1A). The electrodes were either 260 or 520 μm in diameter and were arranged in an alternating checkerboard pattern with 800 μm center-to-center separation between each electrode. As has been described in several papers,[36,44,45] pulse train signals were generated and sent to an external signal processor with custom software. Power and signal information were sent from this processor through a wire to an external transmitter coil that attached magnetically to and communicated inductively with a secondary coil that was implanted subdermally in the subject's temporal skull (Fig. 1B). Power and signal information were sent from this secondary coil through a subdermally implanted wire that traversed the sclera to the array of electrodes. The timing and current of electrical pulses on each electrode were controlled independently.

Psychophysical Methods

All pulse waveforms consisted of trains of biphasic, cathodic-first, and square-wave pulses. For safety reasons, all individual pulses within a pulse train were charge balanced. In this study, we used cathodic and anodic pulses of equal width (0.45 ms, chosen to maximize energy efficiency), with the cathodic phase presented first.[46,47] Each biphasic pulse within the pulse train consisted of a cathodic 0.45-ms pulse, followed by 0.45-ms interphase delay and a 0.45-ms anodic pulse for charge balancing purposes. The biphasic pulse was followed by an 18.65-ms delay before the cathodic phase of the next pulse (totaling 20 ms/50 Hz). The frequency of 50 Hz was chosen to be above the critical flicker fusion frequency of our patients.[36] Pulse trains were 500 ms in duration. All stimuli were presented in photopic conditions. The effect of changing these parameters was not examined. Data collected on single electrodes[34,36] and examinations of spatiotemporal interactions[35] suggest that modifying these parameters would affect sensitivity, but would not fundamentally alter the pattern of the results reported herein.

Subjective Brightness Matching during Paired-Electrode Stimulation

Subjective brightness matching was performed within a given electrode pair, in a two-interval, forced-choice procedure with constant stimuli. Each trial contained two temporal intervals, with an auditory cue marking the onset of each interval. The order of presentation of the two temporal intervals was randomized, and subjects were asked to report which interval contained the brighter stimulus. Each measured data point in the psychometric function was based on a minimum of 12 trials. Additional trials were run, if needed, to improve the fit of the psychometric function up to a maximum of 20 trials per data point (see Supplementary Fig. S1, http://www.iovs.org/lookup/suppl/doi:10.1167/iovs.10-5282/-/DC1, for examples of psychometric functions).

One interval always contained the standard stimulus, which consisted of synchronized pulse trains across the pair of electrodes, Figure 1Ci. The amplitudes of these synchronized pulse trains were set to 1.5, 2, 2.5, or 3 times the perceptual threshold of each electrode in the pair (see Ref. 33 for a detailed description of threshold measurement methods).

The second interval contained the test stimulus, which was identical with the standard except for a temporal phase shift between pulses across the electrode pair (Fig. 1Cii). In those conditions in which both electrodes were stimulated (*conditions 3-5*), we measured brightness matches using pulse trains that were phase shifted by 0.075, 0.375, 1.8, or 9 ms. At our stimulation frequency (50 Hz), a 9-ms phase shift resulted in pulses that were almost perfectly interleaved across the pair of electrodes (Fig. 1Cii).

For each phase shift, brightness-matching psychometric functions were collected for five conditions (Fig. 1D): *Condition 1* consisted of stimulation of electrode (E)1 only, with a range of amplitudes that ranged between 1.5 and 3 times threshold: For example, E1 took 11 values between 90 and 200 μA: 90, 97, 106. . . 200 μA (intervals were chosen on an exponential scale), and E2 = 0 μA. *Condition 2* consisted of stimulation of E2 only: For example, E1 = 0 μA, and E2 took 11 values between 90 and 200 μA: 90, 97, 106. . . 200 μA. In *condition 3*, the amplitude of E1 was fixed (at two to three times threshold), and the amplitude of E2 varied: For example, E1 = 73 μA, whereas E2 varied between 151 and 163 μA. In *condition 4*, the amplitude of E2 was fixed (at two to three times threshold), and E1 varied: For example, E1 varied between 151 and 163 μA, and E2 = 73 μA. Finally, in *condition 5*, the amplitudes of E1 and E2 were jointly varied by multiplicatively scaled amplitude steps: For example, if we were measuring brightness matches at two times threshold and the threshold of E1 was 50 and that of E2 was 100, then E1 would take the amplitudes of 100, 105, 110…150 μA and E2 the corresponding amplitude values of 200, 210, 220…300 μA.

In *conditions 1* to *4*, a cumulative normal based on E1 or E2 alone was used to find the point of subjective equibrightness. In *condition 5*, the cumulative normal was fit based on E1, and the corresponding threshold for E2 was calculated analytically. Example psychometric fits for *condition 5* are shown in Supplementary Figure S1, http://www.iovs.org/lookup/suppl/doi:10.1167/iovs.10-5282/-/DCSupplemental. Error bars were estimated by using an adaptive sampling Monte Carlo simulation.[48] Each psychometric function was inspected to make sure that an adequate fit was obtained, and additional data were collected if fits were inadequate (based either on the estimated error or visual inspection).

Stimulus Set

Measurements were taken for electrode pairs separated by 800 μm (Fig. 2; a total of nine electrode pairs across both subjects), 1600 μm

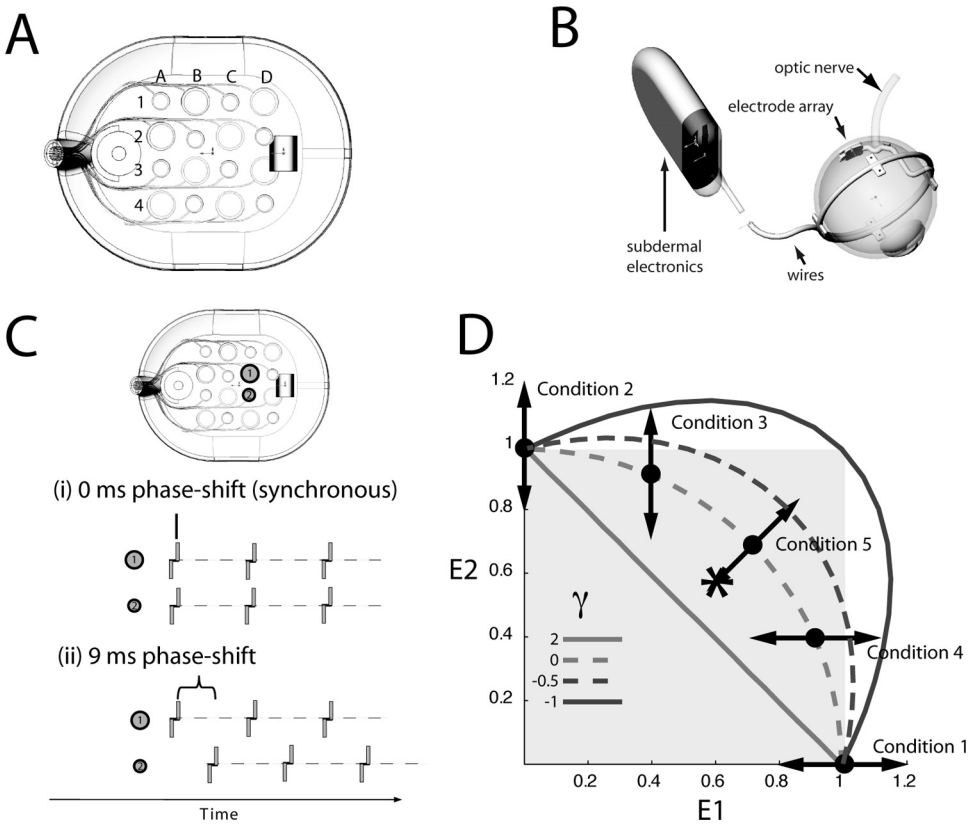

FIGURE 1. (**A**) Electrode array. The electrode array consisted of 260- or 520-μm electrodes arranged in a checkerboard pattern, with center-to-center separation of 800 μm. (**B**) Prosthesis. Stimuli were programmed in a computer program (MatLab; The MathWorks, Natick, MA) that then communicated parameters to an external visual processing unit (not shown). Power and signal information could be independently controlled for each electrode. Panels (**A**) and (**B**) previously published in Horsager A, Greenwald SH, Weiland JD, et al. Predicting visual sensitivity in retinal prosthesis patients. *Invest Ophthalmol Vis Sci*. 2009;50:1483–1491. © ARVO. (**C**) Brightness matching task. Subjects compared the brightness of standard (i) and test (ii) pulse trains. In the case of the standard, the pulses were presented simultaneously across the two electrodes. The test stimulus was identical with the standard, except that there was a phase shift between pulses across the electrode pair. A 9-ms phase shift is shown. Brightness-matching data were collected for phase shifts of 0.075, 0.375, 1.8, and 9 ms. (**D**) Brightness-matching conditions. For each phase shift, brightness-matching psychometric functions were collected in five conditions where the amplitude of E1 (conditions 1 and 4), E2 (conditions 2 and 3), or both E1 and E2 (condition 5) varied, as represented by *double-headed arrows*. The *solid black circles* represent the point of brightness match: the amplitudes at which the apparent brightness of the test stimulus matched the brightness of the standard (✱). Model isobrightness curves are shown for $\gamma = -1$, -0.5, 0, and 2. *Shaded area*: the region of $E_1' \leq 1$ and $E_2' \leq 1$ This is a theoretical data set used for illustrative purposes.

(Fig. 3; four electrode pairs, S06 only), and 2400 μm (Fig. 3; two electrode pairs, S06 only). The only criterion used to choose the electrode pairs was a relatively low single-pulse threshold on both electrodes in the pair. This method allowed us to collect suprathreshold data across a range of brightness levels while remaining within charge safety limits. Given this constraint, electrode pairs were then chosen so that they were distributed as evenly as possible across the array.

The data presented represent ~3-hour testing sessions that occurred roughly once a week over the course of 2 years. Data collection on subject S05 was curtailed before the end of all experiments due to lifting and translating of the array during a surgical procedure (June 2008). This lifting and translating of the array led to a sharp increase in thresholds (in many cases, too high to measure) that made it impossible to continue psychophysical data collection.

Model of Spatiotemporal Integration

Data were fit by using the following model:

$$B = E_1' + E_2' + \gamma E_1' E_2' \qquad (1)$$

The equation describes isobrightness lines that form an ellipse, where B represents the brightness of the percept generated by the standard stimulus on the electrode pair and was fixed to equal 1. E_1' and E_2' represent normalized (as indicated by the prime symbol) current amplitudes for the test stimulus on each of the two electrodes in the pair. Normalization was performed by dividing the current amplitudes on E1 and E2 by the current needed to match the brightness of the standard when using E1 or E2 alone. This normalization forces the isobrightness curves generated by the model to cross the x-axis at $E_2' = 1$ and the y-axis at $E_2' = 1$. This model is closely related to those developed by Rashbass[49] and Watson[39] to describe interactions between luminance pulse pairs as a function of temporal delay in normal vision.

The best fitting value of γ was found for each delay by minimizing the sum of squared errors between the fitted data curve and the obtained values by using unconstrained nonlinear optimization (custom software written in MatLab; The MathWorks, Natick, MA). With stimulation of both electrodes, when $\gamma = 2$, equation 1 reduces to $1 = E_2' + E_2'$, —that is, apparent brightness is proportional to the linear sum of current across both electrodes (Fig. 1D, light gray solid line). This result would be expected if two electrodes stimulated

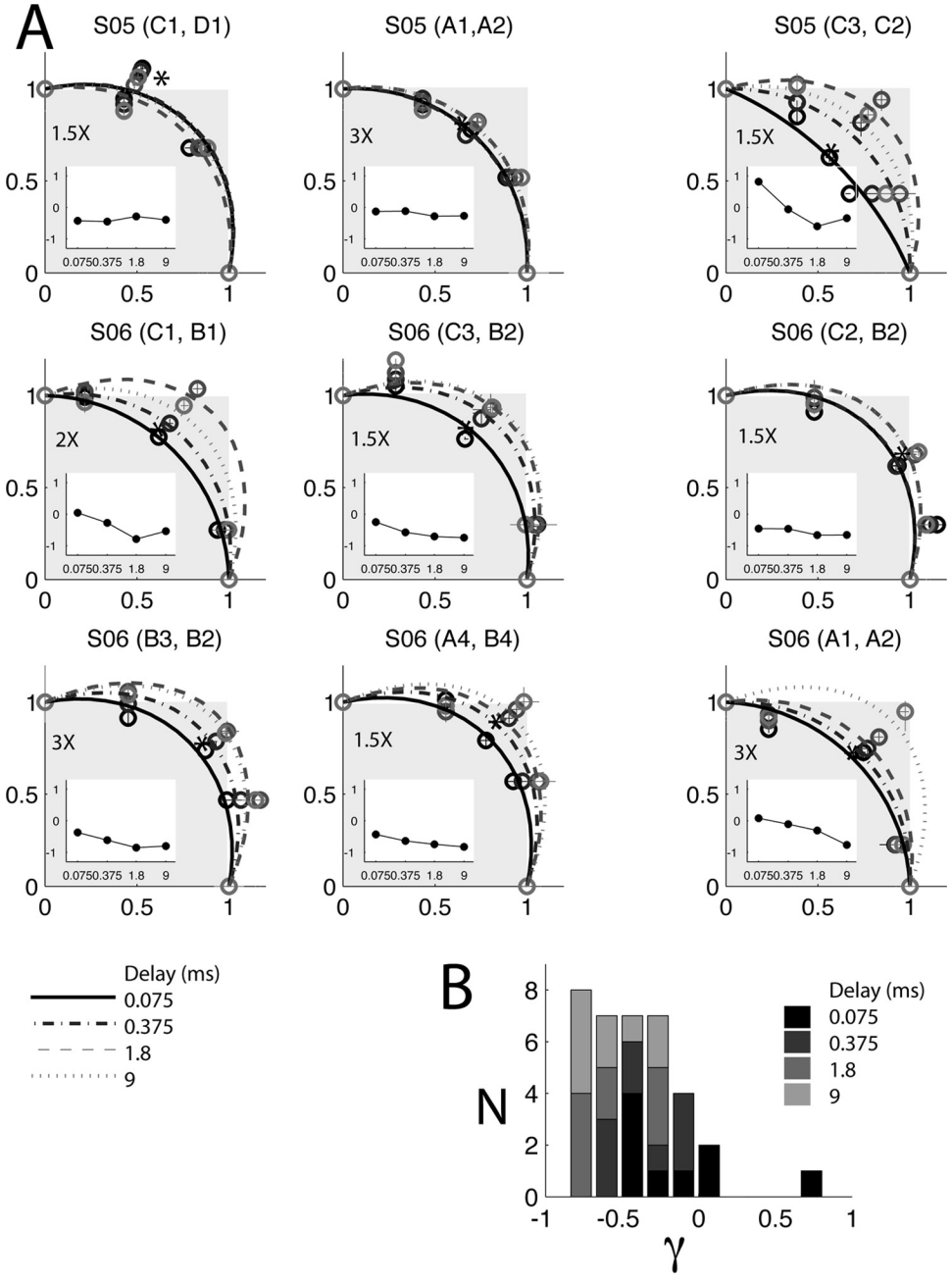

FIGURE 2. **(A)** Isobrightness curves as a function of phase shift for 800-μm-separated electrodes. (✱) The standard stimulus. (○) The point of brightness match. Data and model curves are shown for 0.075 (*black symbols*, *solid lines*), 0.375 (*dark gray symbols*, *dash-dotted lines*), 1.8 (*medium gray symbols*, *dashed lines*), and 9.0 ms (*light gray symbols*, *dotted lines*). *Shading*: the regions of $E_1' \leq 1$ and $E_2' \leq 1$ *Insets*: γ as a function of phase shift. **(B)** The frequency of γ values across all phase shifts and electrode pairs.

exactly the same region in space and time. When $\gamma = 0$, the model simplifies to $1 = E_1'^2 + E_2'^2$ (the equivalent of the equation for a circle) which is the equivalent of adding power across electrodes (Fig. 1D, light gray dashed line).

Inhibition between electrodes can be defined as occurring when the stimulation required of E1 to make a match with the standard is greater when E2 is also stimulated than when E1 alone is stimulated (or vice versa): Brightness matches fall outside the summation area $E_1' \leq 1$ and $E_2' \leq 1$ (Fig. 1D, shaded area). When γ lies between 0 and -1, interaction between electrodes can be considered to be partially suppressive, as shown for $\gamma = -0.5$ (Fig. 1D, dark gray dashed line). Small amounts of current on one electrode result in an inhibitory bowing of the curve outside the summation area $E_1' \leq 1$ and $E_2' \leq 1$ However, when current is distributed more evenly across the two electrodes, there is brightness summation across the pair: The percept is brighter than would be predicted by stimulation of either electrode in isolation.

When γ is less than -1 (Fig. 1D, dark gray, bowed solid line) electrode interactions are fully inhibitory: The entire isobrightness curve bows out beyond the summation region. Thus, γ represents mutual interaction between electrodes and can describe a range of behaviors between linear summation, nonlinear summation, and mutual suppression.

With an exponent of 2, our equation is a suprathreshold analogue to that used by Rashbass[49] to describe threshold interactions between pulse pairs of like and opposite signed contrast as a function of delay between the pairs. As related by Rashbass, the behavior described by equation 1 can result from a simple model where visual transients are filtered by an impulse response and then squared and integrated over a longer time interval.

A closely related alternative is the working model of Watson.[39] In that model, it is again assumed that visual transients are filtered by an impulse response. However instead of a simple square, the response is raised to a power β, which is the slope of the psychometric function

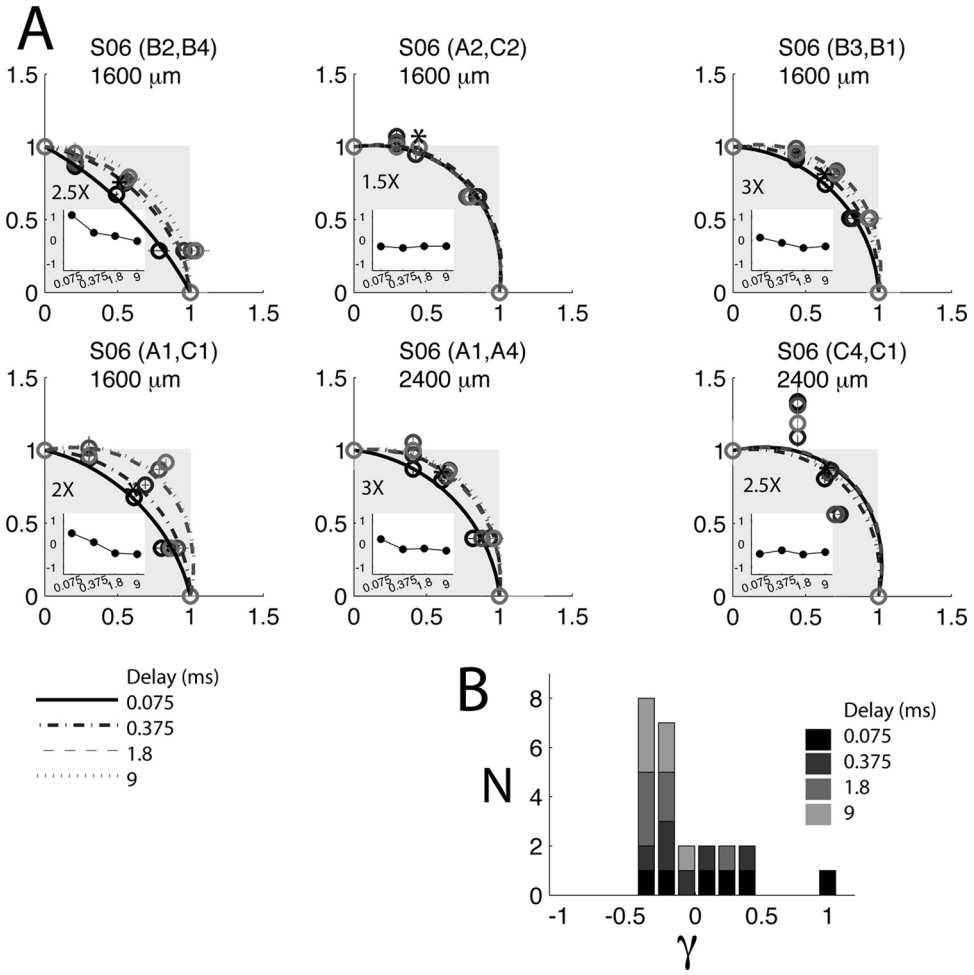

FIGURE 3. (**A**) Isobrightness curves as a function of phase shift for 1600- and 2400-μm-separated electrodes. (✱) The standard stimulus. Data and model curves are shown for 0.075 (*black symbols*, *solid lines*), 0.375 (*dark gray symbols*, *dash-dotted lines*), 1.8 (*medium gray symbols*, *dashed lines*), and 9.0 ms (*light gray symbols*, *dotted lines*) respectively. *Shading*: the regions of $E_2' \leq 1$ and $E_2' \leq 1$ *Insets*: γ as a function of phase shift. (**B**) The frequency of γ values across all phase shifts and electrode pairs.

and typically takes a value between 3 and 6. The second stage of integration takes place over the entire stimulus duration. For the purposes of our dataset, these differences in the temporal properties of the slower second-stage filter are unimportant. We tested the Watson model using a range of exponents and found that it performed similarly to the Rashbass model across a relatively wide of range of exponents (~1.5–4). Variations in the exponent changed the shape of the bowing in a subtle manner and rescaled the γ values, but the resulting isobrightness curves (and mean squared error values) remained very similar to those obtained with an exponent of 2. Since we only had five data points describing the shape of each curve as a function of delay, any attempt to fit the exponent as well as γ caused the model to be underconstrained.

In equation 1, all matches were made to a single brightness level, and B was fixed to equal 1. Our previous findings show that, over the range of amplitudes used in the current paper, the increase in apparent brightness as a function of current on a single electrode is close to linear.[34] This suggests a possible modification of equation 1 to

$$B = (E_1'^2 + E_2'^2 + \gamma E_1' E_2')^{1/2}.$$

With this variant of the model, when the current amplitude on either E1 or E2 is 0, brightness is a linear function of current on the remaining electrode (because B is fixed to 1, the slope is unknown).

RESULTS

As described elsewhere for these patients,[34–36] when a single electrode is stimulated, subjects typically reported that phosphenes appeared white or yellow in color, and were round or oval in shape. At suprathreshold, percepts were reported as being brighter and the perceived shape occasionally became more complex than a simple circle or oval. For single-electrode stimulation, shapes were reported as being approximately 0.5 to 2 inches in diameter at arm's length, corresponding to roughly 1° to 3° of visual angle.

As has also been reported previously,[50] when stimulation was presented on electrode pairs, two different types of percept were obtained. In some cases, the percept was a single phosphene that was reported to be approximately 2 to 4 inches in length/width at arm's length, corresponding to roughly 3° to 6° of visual angle: somewhat larger than the phosphenes produced by a single electrode. On a significant minority of electrode pairs the percept consisted of multiple phosphenes. Although we did not explicitly examine phosphene shape across electrode pairs in this article, previous work on these subjects[50] suggests that when stimulating both electrodes together produces a single percept, the percepts produced by each electrode in isolation are both similar to the shape of the percept produced by paired stimulation (perhaps because both electrodes lie on similar axon pathways). When the phosphene generated by stimulating a pair of electrodes results in two distinct, spatially separated percepts, this percept resembles the composite of the percepts elicited by individual electrode.

Occasionally, a dark rather than a white or yellow percept was reported for a given electrode pair (in these cases the percept was dark across all stimulation timing patterns). In this case, the patient would make a subjective darkness compari-

son. We did not see any systematic differences in threshold or slopes of the brightness-matching psychometric functions between light or dark percepts.

Generally, although the brightness of the perceived stimulus varied as a function of the phase shift—the phenomenon described by our model—the subjects did not report a noticeable difference in the perceived shapes of phosphenes induced by simultaneous versus phase-shifted stimulation (also see Ref. 50). However earlier work by our group examining the effects of timing differences on the appearance of percepts suggests that timing differences (e.g., clockwise versus counterclockwise stimulation across a group of four electrodes) does result in perceptually distinguishable (though not dramatically different) percepts.[35] It is likely that the timing differences manipulated here do result in slight differences in the shape of the elicited percepts, but that these changes in shape are not dramatic enough to be noticed by the subjects or to interfere with the brightness-matching task.

In the brightness-matching task, subjects were asked to ignore all aspects of the percept other than brightness/contrast. As described earlier, percepts could consist either of single or multiphosphenes. In multiphosphene percepts, subjects were asked to average the brightness across all phosphenes. The obtained psychometric functions for these brightness matches (see Supplementary Fig. S1, http://www.iovs.org/lookup/suppl/doi:10.1167/iovs.10-5282/-/DCSupplemental) suggest that subjects were able to perform the task reliably. It is of course possible that subjects were not making a pure brightness judgment (for example, brightness estimates might have been confounded with changes in percept size); however, previous work by our group examining size and brightness judgments as a function of stimulus amplitude on single electrodes suggests that our subjects are capable of making separate judgments of size and brightness,[34] at least when a single electrode is stimulated.

Subjective Brightness as a Function of Pulse Timing across Electrode Pairs

The main panels in Figure 2 show measured brightness matches (symbols) and the best-fitting model isobrightness curves (lines). The inset graphs of each panel represent model estimates of γ as a function of phase shift. The histogram shows the best-fitting values of γ across all electrode pairs and phase shifts. Best fitting estimates of γ and mean squared errors of the model fits are shown in Table 1.

The median estimate of γ was -0.44 for electrodes separated by 800 μm, and most estimates of γ (33/36 estimates: nine electrode pairs $\times$ four phase shifts) fell between 0 and -1, implying *partial suppression* across the electrodes. The mean of the distribution of estimates of γ was significantly less than 0 (two-tailed *t*-test, $P < 0.001$). Across most electrode pairs and phase shifts, the apparent brightness of a percept elicited by E1 was reduced by the presence of a small amount of current on E2, indicated by the data and curves falling outside the shaded region. However, when current was distributed more evenly across the two electrodes, the percept was brighter than would be predicted by stimulation of either electrode in isolation, as indicated by the curves falling inside the shaded region.

In six of the nine electrode pairs, the amount of current needed to match the brightness of the standard increased as a function of phase shift, as represented by the curves' bowing out farther as a function of phase shift in the main panels and a decrease in γ as a function of delay in the inset panels. In the remaining three electrode pairs, the amount of current needed to match the brightness of the standard did not change as a function of delay. This tendency toward a decline in γ as a function of delay implies that mutual inhibition between electrodes increases as a function of delay.

Table 1. Parameters for Model Fits for Electrode Pairs Separated by 800 μm

Subject	E1	E2	Phase-Shift (ms)	γ	Error
S05	C1	D1	0.075	−0.43	0.069
			0.375	−0.45	
			1.8	−0.28	
			9.0	−0.4	
	A1	A2	0.075	−0.13	0.0095
			0.375	−0.12	
			1.8	−0.28	
			9.0	−0.27	
	C3	C2	0.075	0.82	0.0515
			0.375	−0.06	
			1.8	−0.6	
			9.0	−0.34	
S06	C1	B1	0.075	0.04	0.0205
			0.375	−0.28	
			1.8	−0.79	
			9.0	−0.54	
	C3	B2	0.075	−0.25	0.0336
			0.375	−0.58	
			1.8	−0.71	
			9.0	−0.75	
	C2	B2	0.075	−0.46	0.0425
			0.375	−0.46	
			1.8	−0.66	
			9.0	−0.66	
	B3	B2	0.075	−0.37	0.0175
			0.375	−0.62	
			1.8	−0.85	
			9.0	−0.8	
	A4	B4	0.075	−0.43	0.038
			0.375	−0.64	
			1.8	−0.74	
			9.0	−0.83	
	A1	A2	0.075	0.08	0.082
			0.375	−0.1	
			1.8	−0.31	
			9.0	−0.77	

Column 1 shows the identifiers of the two subjects. Columns 2 and 3 list the electrode pairs. Column 4 lists the phase-shift. Column 5 lists the best-fitting γ parameter values. Column 6 lists the sum of squared errors of the model fits.

In seven of the nine electrode pairs, the isobrightness curve for the 0.075 phase shift (Fig. 2, solid line) overlapped or nearly overlapped the data point (Fig. 2, asterisk) representing the standard stimulus (where the pulses were presented simultaneously). For most electrode pairs, the apparent brightness produced by simultaneous stimulation was similar to that produced by stimulation across electrode pairs that was offset by a small phase shift.

It might be expected that, since the size of the current field increases as a function of increasing current amplitude, we would see an increase in spatiotemporal interactions at higher amplitudes or for stimuli farther above threshold. However, we found no effect of pulse amplitude on spatiotemporal integration: similar γ values were found at 1.5, 2, and 3 times threshold, with no statistically significant difference between estimates of γ as a function of threshold multiple using a two-way ANOVA (electrode pair $\times$ threshold multiple, $P > 0.05$).

Figure 3 and Table 2 show data and model fits for electrode pairs separated by 1600 and 2400 μm for S06 only (S05 was unavailable for testing in these conditions, as mentioned earlier). Data were fit with the same model as was used for the 800-μm-separated data.

TABLE 2. Parameter values for model fits for electrode pairs separated by 1600 and 2400 μm in Subject S06

Experiment	E1	E2	Phase-Shift (ms)	γ	Error
1600	B2	B4	0.075	1.07	0.209
			0.375	0.32	
			1.8	0.17	
			9.0	−0.04	
	A2	C2	0.075	−0.27	0.0134
			0.375	−0.33	
			1.8	−0.26	
			9.0	−0.26	
	B3	B1	0.075	0.11	0.066
			0.375	−0.12	
			1.8	−0.34	
			9.0	−0.26	
	A1	C1	0.075	0.45	0.0603
			0.375	0.07	
			1.8	−0.4	
			9.0	−0.44	
2400	A1	A4	0.075	0.2	0.0212
			0.375	−0.23	
			1.8	−0.2	
			9.0	−0.3	
	C4	C1	0.075	−0.42	0.3714
			0.375	−0.27	
			1.8	−0.44	
			9.0	−0.34	

Column 1 lists the distance between electrode pairs. Columns 2 and 3 list the electrode pair. Column 4 lists the phase-shift. Column 5 lists best-fitting λ parameter values. Column 6 lists the sum of squared errors of the model fits.

Estimates of γ were higher for widely separated electrodes: The median value of γ was −0.26, all but one of the 24 (six electrode pairs × four phase shifts) estimates of γ fell between −0.5 and 0.5, and the mean of the distribution of estimates of γ did not differ significantly from 0 (two-tailed *t*-test, $P > 0.05$). Thus, these data support the notion that interactions between electrodes become smaller as a function of electrode separation.

In three of the six electrode pairs the amount of current needed to match the brightness of the standard increased as a function of phase shift, as represented by the curves' bowing out farther as a function of phase shift in the main panels and a decrease in γ as a function of delay in the inset panels. In the remaining three electrode pairs, the amount of current needed to match the brightness of the standard did not change as a function of delay.

For all electrode pairs the curve for the 0.075-ms phase shift overlapped or nearly overlapped the data point representing the standard stimulus (where the pulses were presented simultaneously). Across all the electrode pairs that we tested, the apparent brightness produced by simultaneous stimulation was close to that produced by stimulation offset by a small phase shift.

DISCUSSION

Our earlier work demonstrated significant interactions between pairs of electrodes, even when stimulated nonsimultaneously.[35] In the present study, we examined how these interactions affect perceived brightness by measuring and modeling the current needed to match the brightness of a standard as a function of the temporal separation between suprathreshold electrical pulses across pairs of electrodes.

For electrodes separated by 800 μm, the brightness of the percept produced by stimulating a pair of electrodes depends not only on the current amplitude on each electrode, but also on the timing of stimulation across electrodes: Even when electric fields are not overlapping in time, neural spatiotemporal mechanisms of integration still play a role. As might be expected, spatiotemporal interactions decreased with electrode separation; indeed, the mean of the distribution of estimates of γ did not differ significantly from 0 for electrodes separated by 1600 or 2400 μm.

One possibility is that these effects are mediated by neural populations that lie between, and receive stimulation from, more than one electrode (this neural population might consist of cell bodies, axons, or some combination of the two). Our work examining spatiotemporal interactions is consistent with this hypothesis,[35] although other potential causes of spatiotemporal interactions cannot be excluded. For example, as we have described,[35] recent evidence suggests very fine temporal sensitivity within lateral connections mediated by wide-field amacrine cells whose connections can span up to many millimeters within the retina.[51,52] These connections have the spatial and temporal qualities that would allow integration of current across multiple electrodes. Alternatively, it is possible that these interactions are mediated by cortical sensitivity to precise timing patterns across space. Stimulation with extremely short pulses (~0.1 ms) results in single spikes within ganglion cells that are phase locked to the pulses with high precision.[53,54] If this precise timing information is passed from retina to cortex, as suggested by data showing behavioral adaptation to very high temporal frequencies,[55] it is possible that the sensitivity to pulse timing across electrodes found herein may be the result of cortical mechanisms.

For reasons that are not yet clear, there was significant variability in the estimates of γ across electrode pairs. We saw no clear relationship between estimates of γ and electrode-to-tissue distance or the position of electrode pairs with respect to the macula, although our limited dataset means that we cannot exclude the possibility that these two factors play a role. Other possible sources of variation between electrode pairs include heterogeneity in retinal rewiring or degeneration across the retinal surface.

Although increasing amplitude increased the perceived brightness of both the standard and the test stimuli, the timing of spatiotemporal integration did not vary as a function of amplitude (e.g., 1.5, 2, or 3 times threshold). Although we did not find an effect of amplitude level in our data set, it is likely that interactions between the effects of electrode separation and amplitude levels do occur, given that the neural area of activation is likely to increase with increasing amplitude. However, our data suggest that amplitude levels do not affect the timing of spatiotemporal interactions, consistent with previous work by our group examining the effects of stimulus timing sensitivity within single electrodes.[36]

Previous studies of these patients by our group have demonstrated that it is possible to model perceived brightness as a function of electrical stimulation of a single electrode across a wide variety of timing configurations.[34,36] The model described herein extends this work by modeling spatiotemporal interactions across electrodes. Such spatiotemporal models are, of course, necessary to accurately represent a dynamic visual scene that is constantly changing, both in space and time.

Although it is probable that the model fits that we have described could be improved on with more complex models, the simplicity of our model has the advantage that it requires a relatively small amount of data to be collected to estimate the necessary parameters. Indeed, for a fixed phase shift and brightness level, the model describes brightness as a function

of multiple amplitude levels across both electrodes using a single free parameter. Given earlier work by our group showing that apparent brightness can be described as a power function of stimulation intensity[34] it is likely that this, or a related model, could easily be extended toward describing spatiotemporal interactions across multiple brightness levels. Simple approximation models, such as that described herein, may be of more practical use when designing stimulation protocols that involve multielectrode arrays than the more complex models that require the estimation of a larger number of parameters.

References

1. Bunker CH, Berson EL, Bromley WC, Hayes RP, Roderick TH. Prevalence of retinitis pigmentosa in Maine. *Am J Ophthalmol.* 1984;97:357–365.
2. Heckenlively JR, Foxman SG, Parelhoff ES. Retinal dystrophy and macular coloboma. *Doc Ophthalmol.* 1988;68:257–271.
3. Chader GJ. Animal models in research on retinal degenerations: past progress and future hope. *Vision Res.* 2002;42:393–399.
4. Congdon N, O'Colmain B, Klaver CC, et al. Causes and prevalence of visual impairment among adults in the United States. *Arch Ophthalmol.* 2004;122:477–485.
5. Marc RE, Jones BW. Retinal remodeling in inherited photoreceptor degenerations. *Mol Neurobiol.* 2003;28:139–147.
6. Jones BW, Watt CB, Marc RE. Retinal remodelling. *Clin Exp Optom.* 2005;88:282–291.
7. Mazzoni F, Novelli E, Strettoi E. Retinal ganglion cells survive and maintain normal dendritic morphology in a mouse model of inherited photoreceptor degeneration. *J Neurosci.* 2008;28:14282–14292.
8. Santos A, Humayun MS, de Juan E Jr, et al. Preservation of the inner retina in retinitis pigmentosa: a morphometric analysis. *Arch Ophthalmol.* 1997;115:511–515.
9. Humayun MS, Prince M, de Juan E Jr, et al. Morphometric analysis of the extramacular retina from postmortem eyes with retinitis pigmentosa. *Invest Ophthalmol Vis Sci.* 1999;40:143–148.
10. Lagali PS, Balya D, Awatramani GB, et al. Light-activated channels targeted to ON bipolar cells restore visual function in retinal degeneration. *Nat Neurosci.* 2008;11:667–675.
11. Margolis DJ, Newkirk G, Euler T, Detwiler PB. Functional stability of retinal ganglion cells after degeneration-induced changes in synaptic input. *J Neurosci.* 2008;28:6526–6536.
12. Stasheff SF. Emergence of sustained spontaneous hyperactivity and temporary preservation of OFF responses in ganglion cells of the retinal degeneration (rd1) mouse. *J Neurophysiol.* 2008;99:1408–1421.
13. Bainbridge JW, Smith AJ, Barker SS, et al. Effect of gene therapy on visual function in Leber's congenital amaurosis. *N Engl J Med.* 2008;358:2231–2239.
14. Hauswirth WW, Aleman TS, Kaushal S, et al. Treatment of leber congenital amaurosis due to RPE65 mutations by ocular subretinal injection of adeno-associated virus gene vector: short-term results of a phase I trial. *Hum Gene Ther.* 2008;19:979–990.
15. Cideciyan AV, Aleman TS, Boye SL, et al. Human gene therapy for RPE65 isomerase deficiency activates the retinoid cycle of vision but with slow rod kinetics. *Proc Natl Acad Sci U S A.* 2008;105:15112–15117.
16. Cideciyan AV, Hauswirth WW, Aleman TS, et al. Human RPE65 gene therapy for Leber congenital amaurosis: persistence of early visual improvements and safety at 1 year. *Hum Gene Ther.* 2009;20:999–1004.
17. Cideciyan AV, Hauswirth WW, Aleman TS, et al. Vision 1 year after gene therapy for Leber's congenital amaurosis. *N Engl J Med.* 2009;361:725–727.
18. Banghart M, Borges K, Isacoff E, Trauner D, Kramer RH. Light-activated ion channels for remote control of neuronal firing. *Nat Neurosci.* 2004;7:1381–1386.
19. Chambers JJ, Banghart MR, Trauner D, Kramer RH. Light-induced depolarization of neurons using a modified Shaker K(+) channel and a molecular photoswitch. *J Neurophysiol.* 2006;96:2792–2796.
20. Szobota S, Gorostiza P, Del Bene F, et al. Remote control of neuronal activity with a light-gated glutamate receptor. *Neuron.* 2007;54:535–545.
21. Nagel G, Szellas T, Huhn W, et al. Channel rhodopsin-2, a directly light-gated cation-selective membrane channel. *Proc Natl Acad Sci U S A.* 2003;100:13940–13945.
22. Boyden ES, Zhang F, Bamberg E, Nagel G, Deisseroth K. Millisecond-timescale, genetically targeted optical control of neural activity. *Nat Neurosci.* 2005;8:1263–1268.
23. Bi A, Cui J, Ma YP, et al. Ectopic expression of a microbial-type rhodopsin restores visual responses in mice with photoreceptor degeneration. *Neuron.* 2006;50:23–33.
24. Lin B, Koizumi A, Tanaka N, Panda S, Masland RH. Restoration of visual function in retinal degeneration mice by ectopic expression of melanopsin. *Proc Natl Acad Sci U S A.* 2008;105:16009–16014.
25. Daiger SP, Bowne SJ, Sullivan LS. Perspective on genes and mutations causing retinitis pigmentosa. *Arch Ophthalmol.* 2007;125:151–158.
26. Schnapf JL, Kraft TW, Baylor DA. Spectral sensitivity of human cone photoreceptors. *Nature.* 1987;325:439–441.
27. Wang H, Peca J, Matsuzaki M, et al. High-speed mapping of synaptic connectivity using photostimulation in Channelrhodopsin-2 transgenic mice. *Proc Natl Acad Sci U S A.* 2007;104:8143–8148.
28. Humayun MS, de Juan E Jr, Weiland JD, et al. Pattern electrical stimulation of the human retina. *Vision Res.* 1999;39:2569–2576.
29. Rizzo JF, III, Wyatt J, Loewenstein J, Kelly S, Shire D. Perceptual efficacy of electrical stimulation of human retina with a microelectrode array during short-term surgical trials. *Invest Ophthalmol Vis Sci.* 2003;44:5362–5369.
30. Weiland JD, Yanai D, Mahadevappa M, et al. Visual task performance in blind humans with retinal prosthetic implants. *Conf Proc IEEE Eng Med Biol Soc.* 2004;6:4172–4173.
31. Yanai D, Weiland JD, Mahadevappa M, Greenberg RJ, Fine I, Humayun MS. Visual performance using a retinal prosthesis in three subjects with retinitis pigmentosa. *Am J Ophthalmol.* 2007;143:820–827.
32. Zrenner E. *Subretinal Implants for the Restitution of Vision in Blind Patients.* Presented at the annual meeting of the Association for Research in Vision and Ophthalmology, Fort Lauderdale, Florida, May 6, 2007.
33. de Balthasar C, Patel S, Roy A, et al. Factors affecting perceptual thresholds in epiretinal prostheses. *Invest Ophthalmol Vis Sci.* 2008;49:2303–2314.
34. Greenwald SH, Horsager A, Humayun MS, Greenberg RJ, McMahon MJ, Fine I. Brightness as a function of current amplitude in human retinal electrical stimulation. *Invest Ophthalmol Vis Sci.* 2009;50:5017–5025.
35. Horsager A, Greenberg RJ, Fine I. Spatiotemporal interactions in retinal prosthesis subjects. *Invest Ophthalmol Vis Sci.* 2010;51:1223–1233.
36. Horsager A, Greenwald SH, Weiland JD, et al. Predicting visual sensitivity in retinal prosthesis patients. *Invest Ophthalmol Vis Sci.* 2009;50:1483–1491.
37. Chader GJ, Weiland J, Humayun MS. Artificial vision: needs, functioning, and testing of a retinal electronic prosthesis. *Prog Brain Res.* 2009;175:317–332.
38. Stevens SS. On the psychophysical law. *Psychol Rev.* 1957;64:153–181.
39. Watson AB. Temporal Sensitivity. In: Boff K, Kaufman L, Thomas J, eds. *Handbook of Perception and Human Performance*. New York: Wiley; 1986.
40. Boex C, de Balthasar C, Kos MI, Pelizzone M. Electrical field interactions in different cochlear implant systems. *J Acoust Soc Am.* 2003;114:2049–2057.
41. Stickney GS, Loizou PC, Mishra LN, Assmann PF, Shannon RV, Opie JM. Effects of electrode design and configuration on channel interactions. *Hear Res.* 2006;211:33–45.
42. Wilson BS, Finley CC, Lawson DT, Wolford RD, Zerbi M. Design and evaluation of a continuous interleaved sampling (CIS) processing strategy for multichannel cochlear implants. *J Rehabil Res Dev.* 1993;30:110.

43. de Balthasar C, Boex C, Cosendai G, Valentini G, Sigrist A, Pelizzone M. Channel interactions with high-rate biphasic electrical stimulation in cochlear implant subjects. *Hear Res.* 2003;182:77–87.
44. Humayun MS, Weiland JD, Fujii GY, et al. Visual perception in a blind subject with a chronic microelectronic retinal prosthesis. *Vision Res.* 2003;43:2573–2581.
45. Mahadevappa M, Weiland JD, Yanai D, Fine I, Greenberg RJ, Humayun MS. Perceptual thresholds and electrode impedance in three retinal prosthesis subjects. *IEEE Trans Neural Syst Rehabil Eng.* 2005;13:201–206.
46. Loeb GE, White MW, Jenkins WM. Biophysical considerations in electrical stimulation of the auditory nervous system. *Ann N Y Acad Sci.* 1983;405:123–136.
47. Jensen RJ, Ziv OR, Rizzo JF. Responses of rabbit retinal ganglion cells to electrical stimulation with an epiretinal electrode. *J Neural Eng.* 2005;2:S16–S21.
48. Wichmann FA, Hill NJ. The psychometric function: II. Bootstrap-based confidence intervals and sampling. *Percept Psychophys.* 2001;63:1314–1329.
49. Rashbass C. The visibility of transient changes of luminance. *J Physiol.* 1970;210:165–186.
50. Nanduri D, Humayun MS, Greenberg RJ, McMahon MJ, Weiland JD. Retinal prosthesis phosphene shape analysis. *Conf Proc IEEE Eng Med Biol Soc.* 2008;2008:1785–1788.
51. Amthor FR, Tootle JS, Grzywacz NM. Stimulus-dependent correlated firing in directionally selective retinal ganglion cells. *Vis Neurosci.* 2005;22:769–787.
52. Baccus SA. Timing and computation in inner retinal circuitry. *Annu Rev Physiol.* 2007;69:271–290.
53. Fried SI, Hsueh HA, Werblin FS. A method for generating precise temporal patterns of retinal spiking using prosthetic stimulation. *J Neurophysiol.* 2006;95:970–978.
54. Sekirnjak C, Hottowy P, Sher A, Dabrowski W, Litke AM, Chichilnisky EJ. High-resolution electrical stimulation of primate retina for epiretinal implant design. *J Neurosci.* 2008;28:4446–4456.
55. Shady S, MacLeod DI, Fisher HS. Adaptation from invisible flicker. *Proc Natl Acad Sci U S A.* 2004;101:5170–5173.